Bulk Negative Differential Conductivity in Germanium: Theory

Abstract: Two mechanisms have been proposed^{6,7} for the bulk negative differential conductivity of n-type germanium first observed by Elliott et al.² These are discussed with reference to recent Monte Carlo calculations in which effects due to intravalley acoustic phonon scattering, $\langle 100 \rangle$ and $\langle 000 \rangle$ minima and ellipsoidal constant energy surfaces are explored. Strong evidence is presented that electron transfer to $\langle 100 \rangle$ minima causes this negative conductance. The origin of its temperature and orientation dependence is discussed.

Introduction

Bulk negative differential conductivity (BNDC) has been observed in n-type germanium under a wide variety of conditions, for example,

- (1) in gold-doped material at 77°K,¹
- (2) in fairly pure material below 150°K, 2,3
- (3) in fairly pure material under uniaxial stress at 300°K and below, and
- (4) in very pure material at 4°K.5

These observations originate from different mechanisms. The first is due to the field-dependent capture cross-section of gold ions for electrons. The third is due to a field-induced transfer of electrons between $\langle 111 \rangle$ minima split by the unaxial stress. The fourth is almost certainly due to a field-induced transfer of electrons between $\langle 111 \rangle$ minima under exceptional intervalley scattering conditions. Controversy surrounds the origin of the second; one suggestion is that it originates from a field-induced transfer of electrons to higher ($\langle 100 \rangle$) minima, another is that it is due to acoustic phonon scattering under conditions for which spontaneous emission is important.

This paper will be devoted to a consideration of the origin of the second BNDC^{2,3} effect listed above. This effect is of particular significance because it occurs in what we may refer to as normal material and is observed under usual conditions. The main features of this BNDC are (a) it is observed only below 150°K, increasing as the temperature is lowered; (b) even at low temperature (27°K) is small by comparison with effects in gallium arsenide; (c) it is orientation dependent, being observed with electric field vector **E** parallel to $\langle 100 \rangle$ but not for **E** $\parallel \langle 111 \rangle$; and (d) it is removed by hydrostatic pressure.

Figure 1 Schematic diagram of the conduction band minima of germanium near the energy gap.

First we examine the suggestions put forward for its origin. Figure 1 shows the relative positions of the lowerenergy conduction band minima of germanium. It was suggested some time ago⁹ that population of the $\langle 100 \rangle$ minima was occurring in high electric fields and was responsible for the (then) apparent saturation of drift velocity. More recently it was suggested that this process was the mechanism responsible for the BNDC.6 Calculations based on displaced Maxwellian distribution functions for carriers in the $\langle 100 \rangle$ and $\langle 111 \rangle$ minima did predict BNDC that had the observed temperature dependence and the approximately correct magnitude. However, as mentioned earlier, the BNDC is small and consequently any prediction of it invites criticism of the approximations that are employed. The main approximations introduced were (1) the imposed form of the distribution functions, (2) neglect of the $\langle 000 \rangle$ minimum and (3) representation of the ellipsoidal constant energy

 $[\]begin{array}{c|c} \text{One } \langle 000 \rangle & \text{Six } \langle 100 \rangle \\ \text{minimum} & \\ (\Gamma_2) & \\ \text{Four } \langle 111 \rangle & \\ \text{minima} & \\ (L_1) & \\ \text{Energy gap} & \\ \end{array}$

The author is located at the Royal Radar Establishment, Malvern, Worcestershire, England.

surfaces of the $\langle 111 \rangle$ and $\langle 100 \rangle$ minima by spherical constant-energy surfaces characterized by a density-of-states mass and a conductivity mass.

An alternate suggestion of an intraband effect for the origin of the BNDC was put forward by Dumke, who proposed that the failure of the equipartition of energy approximation for those acoustic phonons involved in scattering high-energy electrons in the $\langle 111 \rangle$ minima was responsible, though no estimates of the effects in germanium are available. Some general analytical expressions are available from the work of Stratton. The failure of their approximation was ignored in the calculations of Fawcett and Paige though it is clear an electron in the $\langle 111 \rangle$ minimum with an energy of 0.2 eV (i.e., sufficient energy to make a transition to the $\langle 100 \rangle$ minimum) can emit a phonon of energy greater than kT at 27°K.

Recently Fawcett and Paige¹¹ carried out a series of calculations in which the various approximations introduced in earlier work were examined and more realistic parameters were used. In particular, the form of the distribution function was not assumed but was calculated by the Monte Carlo method; ellipsoidal constant energy surfaces were introduced for (111) and (100) minima; and the importance of the (100) minimum and intraband acoustic phonon scattering were investigated. The remainder of this paper is devoted to a discussion of that work.

Calculation of the distribution function

We are concerned with calculating the distribution function associated with a minimum with ellipsoidal constant energy surfaces. By transformation into w-space where the electron energy, ϵ , is given by

$$\epsilon(w) = \frac{h^2 w^2}{2m_0} \,, \tag{1}$$

 m_0 being the free electron mass, and assuming that all scattering processes are randomizing, the distribution function has cylindrical symmetry about the field \mathbf{E}' , which is the accelerative field in w-space obtained from \mathbf{E} , the field in \mathbf{k} -space, by the transformation

$$\mathbf{E}' = \mathbf{T} \cdot \mathbf{E} \tag{2}$$

where T is defined by the transformation

$$\mathbf{w} = \mathbf{T} \cdot \mathbf{k} \qquad \text{i.e.,}$$

$$\mathbf{T} = \begin{bmatrix} \left(\frac{m_0}{m_1}\right)^{\frac{1}{2}} & 0 & 0 \\ 0 & \left(\frac{m_0}{m_2}\right)^{\frac{1}{2}} & 0 \\ 0 & 0 & \left(\frac{m_0}{m_2}\right)^{\frac{1}{2}} \end{bmatrix}$$
(3)

From the distribution function a mean value, $\langle \mathbf{w} \rangle$, of w

was found. It was transformed to a velocity in real space to find the drift velocity, $\langle \mathbf{v} \rangle$

$$\langle \mathbf{v} \rangle = \frac{\hbar}{m_0} \, \mathbf{T} \langle \mathbf{w} \rangle \tag{4}$$

associated with the minimum. The form of **T** reveals that **E** and $\langle \mathbf{v} \rangle$ were referred to the principal axes of the ellipsoidal constant energy surfaces. In general, further transformations were required to refer **E** and $\langle \mathbf{v} \rangle$ to a common set of crystal axes because the principal axes of the various minima do not coincide.

The Monte Carlo technique which was used to determine the distribution function has been described previously. ¹² In this method, the motion of a single electron through w-space is simulated by generating successive random numbers to represent the time of free flight in the electric field, the scattering mechanism and the final state after scattering. The w-space within each minimum is divided into boxes and the time spent by the electron in each box (the visiting time) is recorded. After many collisions the visiting time in each box is proportional to the distribution function in w-space. The total time spent by the electron in each minimum is proportional to the carrier population in that minimum and is given by $\sum (w_f - w_i) h/eE'$ where w_i and w_f are the initial and final wave vectors of the flight and the summation is over flights in w-space.

In addition to the phonon scattering mechanisms, a "self-scattering" process was included for which the scattering rate between two states \mathbf{w} and \mathbf{w}' in minimum α was taken to be

$$S_{\alpha}(\mathbf{w}, \mathbf{w}') = \left[\Gamma_{\alpha} - \sum_{\mathbf{x}} \lambda_{\alpha s}(\mathbf{w}) \right] \delta(\mathbf{w} - \mathbf{w}')$$
 (5)

where Γ_{α} is a constant and $\lambda_{\alpha s}(\mathbf{w})$ is the total scattering rate for the state \mathbf{w} due to the real scattering process s. While this "self-scattering" is of no physical significance, since it does not change the electron-wave vector, it simplifies the numerical procedure by distributing the times of free flight according to the simple negative exponential distribution $1/\Gamma_{\alpha} \exp{[-\Gamma_{\alpha}t]}$.

When the electron has suffered about 40,000 real collisions in each minimum the distribution function converges and w could be evaluated by numerical integration. In practice, w was not obtained in this way, since the accuracy depends on subdividing w-space into a sufficiently small mesh. Instead the expression

$$\mathbf{w} = \frac{1}{2} \sum (\mathbf{w_f^2 - w_i^2}) / \sum (\mathbf{w_f - w_i})$$

was used where the summations are over flights in w-space.

Band structure and scattering processes

The essential features of the band structure of germanium for the problem in hand are shown in Fig. 1. The $\langle 000 \rangle$ minimum has spherical constant-energy surfaces, while the surfaces of the $\langle 111 \rangle$ and $\langle 100 \rangle$ minima are ellipsoids

563

Table 1 Conduction band parameters of germanium.

Minimum	Number	m_1/m_0	m_t/m_0	Δ (eV)	
111	4	1.577a	0.0815a		
00	i	0.037b	0.037b	0.14^{b}	
0	6	0.90∘	0.1920	0.18^{d}	

^a Ref. 9, page 145.

d Ref. 14.

of revolution. The effective masses and energy separations relative to the $\langle 111 \rangle$ minima are given in Table 1. The $\langle 100 \rangle$ effective masses have been assumed to be identical to those in silicon.

The electric field lowers the crystal symmetry. Two directions of **E** have been considered, **E** || [100] and **E** || [111]. When **E** || [100], all four $\langle 111 \rangle$ minima remain equivalent and a determination of distribution function is necessary for only one of these. However, the $\langle 100 \rangle$ minima form two sets, the [100] and [100] minima in one set, [010], [010], [001] and [001] in the other. These will be referred to as the [100] and [010] sets. Similarly when **E** || [111], all six $\langle 100 \rangle$ minima are equivalent but the [111] minimum must be distinguished from the [111], [111] and

 $[1\overline{1}1]$. These will be referred to as the [111] and $[\overline{1}11]$ sets.

The scattering processes considered have been limited to phonons. They include acoustic and optic intravalley, equivalent intervalley and non-equivalent intervalley. They are listed in Table 2 together with their branch. energy (if they are high energy) and deformation potential,

An approximate treatment of intravalley acoustic phonon scattering for ellipsoidal constant energy surfaces gives a scattering rate

$$\lambda(\epsilon) = \frac{(m_1 m_2 m_3)^{\frac{1}{2}} \Xi_{\text{av}}^2 k T}{\sqrt{2} \pi h^4 \rho s^2} \cdot \epsilon^{\frac{1}{2}}$$
 (6)

where Ξ_{av} is an average deformation potential chosen to give agreement between the zero-field lattice mobility calculated using Eq. (6) and the observed acoustic phonon limited value, ρ is the crystal density, s is the velocity of sound, T is the lattice temperature and k Boltzmann's constant. An approximate treatment of this form for ellipsoidal constant energy surfaces was found necessary to avoid time consuming computation.

Optical and intervalley scattering has been calculated using the usual expressions. Three distinguishable types of equivalent intervalley scattering among (100) minima have been included by analogy with silicon. ¹³

The role of the (000) and (100) minima

First the results of calculations in which the $\langle 000 \rangle$ minimum has been ignored will be presented, followed by results

Table 2 Electron-phonon scattering processes in germanium.

	Minimum			Phonon cuoren		
Type	Initial	Final	Branch	Phonon energy (equivalent temp.)	Ξ_{av} (eV)	D/a (eV/cm)
(111	111	Acoustic		11.8a	
-	111	111	Optic	430 °K		9×10^{8a}
j	000	000	Acoustic		5 ^b	
Intravalley)	000	000	Optic	430 °K		Forbidden
	100	100	Acoustic		7.4°	
· ·	100	100	Optic	430 °K		Forbidden
(111	1 11	Acoustic	320 °K	_	1.6×10^{8d}
Equivalent	100	100	Optic	430 °K	-	1.1×10^{9e}
Intervalley	100	100	Acoustic	100 °K		8.8×10^{7e}
	100	010	Acoustic	320 °K		3.8×10^{8e}
Non-	111	000	Acoustic	320 °K		$2 \times 10^{8 \mathrm{f}}$
Equivalent <	111	100	Acoustic	320 °K		1×10^{8} f
Intervalley	000	100	Acoustic	320 °K		2×10^{8} f

^a Ref 9, page 102.

^b W. Paul, J. Phys. Chem. Solids 8, 196 (1959).

^e C. J. Rauch, J. J. Stickler, H. J. Zeiger and G. S. Heller, *Phys. Rev. Letters* 4, 64 (1960).

^b T. P. McLean and E. G. S. Paige, J. Phys. Chem. Solids, 23, 833 (1962).

[°] Ref. 13.

^d G. Weinreich, T. M. Saunders and H. G. White, *Phys. Rev.* 114, 33 (1959).

See text.

Assumed values.

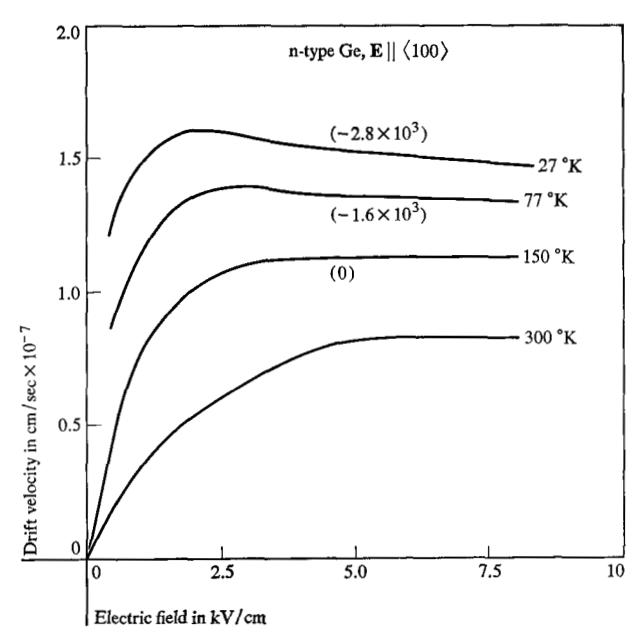


Figure 2 Variation of the drift velocity with field for $\mathbf{E}||\langle 100\rangle|$ at various temperatures. The figures in parentheses are the maximum negative mobilities in units of cm²/V-sec.

which show that the $\langle 000 \rangle$ minimum has an insignificant effect on the mobility.

Calculations have been performed for E || [100] and E | [111]. In both cases three distinguishable sets of minima are required as described above. All minima are ellipsoidal and it is therefore necessary to perform the transformation to w-space for each (see the section on the distribution function). Even with neglect of the $\langle 000 \rangle$ minimum, the number of parameters involved is large. They were selected in the following way; Parameters for the (111) minima are well known and these were taken from the literature (see Tables 1 and 2), the possible exception here being the coupling constant for optical modes. The author has been strongly influenced by the arguments in Ref. 9 in selecting a value for this parameter! Parameters for the (100) are not well known. In the absence of any good experimental evidence, the effective mass parameters have been taken as identical to those for silicon. A value of 900 cm²/V-sec for the mobility in the $\langle 100 \rangle$ minima has been found for germanium subjected to a hydrostatic pressure such that the (100) minima have a lower energy than the (111) minima. 14 From this mobility, the ratio of deformation potentials from silicon¹⁵ and the silicon effective masses, the deformation potentials of Table 2 were obtained. The nonequivalent intervalley deformation potential was treated as an adjustable parameter.

Figure 2 shows the variation of drift velocity with electric field for $\mathbf{E} \mid\mid \langle 100 \rangle$ for various temperatures with a coupling strength of 1×10^8 eV/cm for the adjustable parameter. A BNDC is predicted at low temperature,

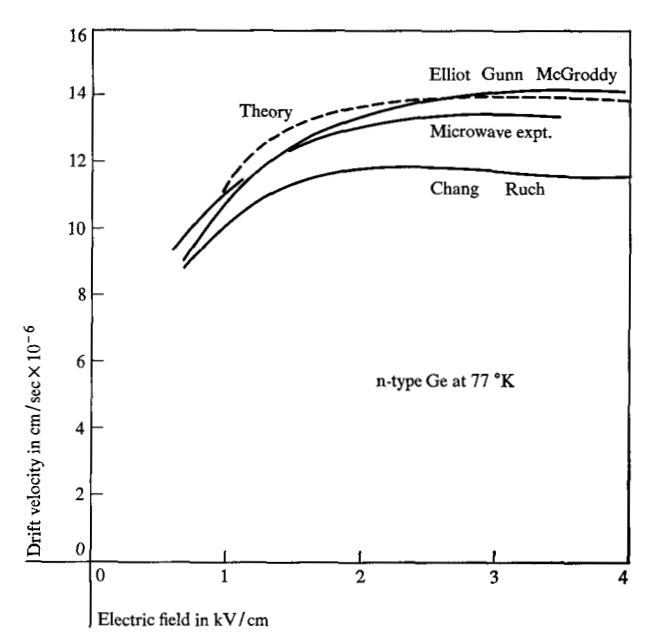


Figure 3 Variation of drift velocity with field for $E||\langle 100\rangle|$ at 77°K showing a comparison between theory and various experimental results. (Low frequency microwave results presented in the paper by A. C. Baynham, p. 568.)

diminishing with increasing temperature, until at 150°K it has disappeared. Values of threshold field, level of drift velocity and magnitude of negative mobility (shown in brackets in Fig. 2) are within the range of experimental results.^{2,3} Figure 3 shows a comparison of theory with experimental results at 77°K.

Having shown that a BNDC can be predicted for $\mathbf{E} \mid\mid \langle 100 \rangle$, it is vital to establish the validity of the model to show that no BNDC occurs when $\mathbf{E} \mid\mid \langle 111 \rangle^*$. Figure 4 shows results for $\mathbf{E} \mid\mid \langle 111 \rangle$ as well as for $\mathbf{E} \mid\mid \langle 100 \rangle$ at 77°K; the $\mathbf{E} \mid\mid \langle 111 \rangle$ results show a positive mobility over the complete field range. The maximum in the anisotropy as measured by the ratio of drift velocities for \mathbf{E} parallel to $\langle 100 \rangle$ and $\langle 111 \rangle$ occurs at about 1 kV/cm and has a value of 1.57 in good agreement with experimental results. ^{16,17} At all temperatures in the 27°K to 300°K range, no BNDC was predicted for $\mathbf{E} \mid\mid \langle 111 \rangle$.

Hydrostatic pressure experiments have been simulated by changing the energy separation between $\langle 100 \rangle$ and $\langle 111 \rangle$ minima. Results at 77°K for an energy separation of 0.117 eV (0.18 eV for zero pressure) are shown in Fig. 4 by the dashed curves. This separation is equivalent to a hydrostatic pressure of 10 kbar. Despite the large distortion of the band structure the effects are modest for $\mathbf{E} \parallel \langle 100 \rangle$ and remarkably small for $\mathbf{E} \parallel \langle 111 \rangle$. The threshold field for BNDC is little affected but a high field limit has appeared in the field range up to 8 kV/cm.

^{*} We refer to the high field results, E > 500 V/cm. The BNDC observed by Kastalskii and Ryvkin, s when E || (111), occurred at very low field strengths, about 5 V/cm, and are not our concern here.

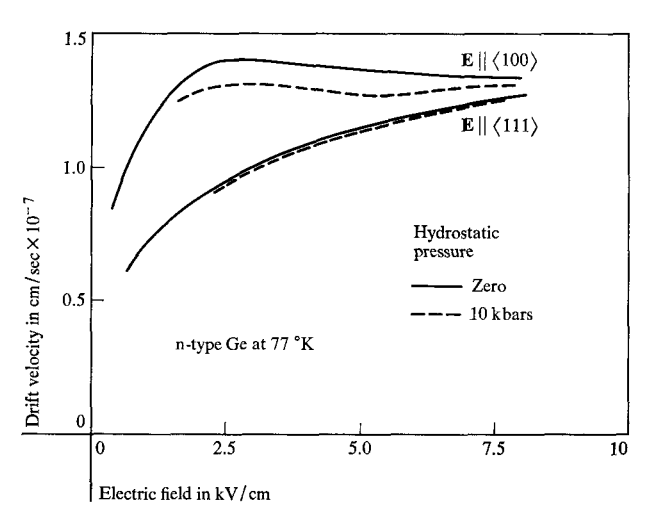


Figure 4 Anisotropy of the BNDC and simulation of the effect of hydrostatic pressure at 77°K.

These results are qualitatively similar to those seen experimentally though the BNDC has disappeared even at a pressure of 4 kbar. The difference may be attributed to an overestimate of the BNDC by the model.

Simulation of uniaxial stress measurements, for a stress collinear with an electric field in the $\langle 100 \rangle$ direction, is possible with the present model but has not yet been investigated.

The importance of the $\langle 000 \rangle$ minimum was investigated by introducing additional approximations into the treatment of the problem in order to confine our considerations to three distinguishable minima. Only the case of $\mathbf{E} \parallel \langle 100 \rangle$ was considered. Then the two distinguishable sets of (100) minima were treated as one suitably averaged set (due to strong equivalent intervalley scattering this is a good approximation). Comparison was then made between velocity-field curve calculations including and excluding the (000) minimum. With the parameters given in Tables 1 and 2 the agreement was within 1\%. It was clear that although the mobility of electrons in the (000) minimum was high (fourfold increase over mobility in $\langle 111 \rangle$ minima), the density-of-states factor rendered them ineffective in influencing the drift velocity (population less than 0.2% of total).

Discussion

These calculations show that a BNDC can exist in n-type germanium due to the presence of $\langle 100 \rangle$ conduction band minima. A comparison with experimental results suggests that the calculation is, if anything, overestimating the magnitude of the BNDC. This overestimate may be remedied by a small increment in the $\langle 111 \rangle$ to $\langle 100 \rangle$ minima scattering rate. In fact, in trying to fit exact expressions to Jayaraman and Kosicki's ¹⁴ zero field, hydrostatic-pressure

measurements we find that the measurements cannot be reproduced without assuming appreciable pressure dependence of mobility in the $\langle 100 \rangle$ minima and a stronger $\langle 111 \rangle$ – $\langle 100 \rangle$ coupling ($|D/a| = 5 \times 10^8$ eV/cm) than used in the preceding calculation. A 20% increase in $\langle 100 \rangle$ masses and this value of $\langle 111 \rangle$ – $\langle 100 \rangle$ coupling still give a negative mobility at 27°K, which at 77°K has become so small that it is indistinguishable from saturation within the error of our present calculations. (The experimentally observed BNDC is also so small that we would not expect to have the necessary accuracy to predict it). Calculations with these parameters are incomplete.

• Origin of temperature dependence:

At zero field, since impurity scattering has been neglected, the low-temperature mobility of $\langle 111 \rangle$ electrons is greater than at a high temperature. Consequently, the rate of gain of energy in an electric field is higher and the mobility falls to a value comparable to that in the higher temperature crystal, but never below it. The mobility of carriers in the \langle 100 \rangle minima shows little dependence on lattice temperature in the 27°K to 150°K range. The consequences of these features are that for the lower lattice temperature (1) the rate of decrease of mobility $(\langle 111 \rangle)$ with field is greater, (2) the peak in the variation of the rate of transfer of electrons from (111) minima to $\langle 100 \rangle$ minima occurs at lower fields, when $(d^2v/dE^2)_{(111)}$ is greatest, and (3) the change in mobility of an electron on transfer from a $\langle 111 \rangle$ to a $\langle 100 \rangle$ minimum is greater. It is this combination of features that leads to the larger BNDC at the lower temperature.

• Origin of orientation dependence.

The orientational dependence of the BNDC originates from the transfer of electrons between minima which are equivalent in the absence of **E**. When **E** || [100] no net transfer of electrons between $\langle 111 \rangle$ minima occurs but there is a weak tendency for the low mobility [100] set of minima to have a higher occupancy than the [010] set (see Fig. 5). This tends to enhance the BNDC. In contrast, when **E** || [111], there is a very large transfer of electrons from the high mobility [111] set to the low mobility [111] set of minima due to the weak intervalley coupling. The rate of transfer with field to the $\langle 100 \rangle$ minima is reduced and the transfer becomes insignificant since electrons in the minimum have a *lower* mobility than in the $\langle 100 \rangle$ minima. This destroys the BNDC as shown in Fig. 4.

• Other sources of BNDC.

Other factors that can contribute to a BNDC are electron transfer from the $\langle 111 \rangle$ minima to impurity states associated with the $\langle 100 \rangle$ minima, non-parabolicity of the $\langle 111 \rangle$ minima and the previously mentioned intra-band acoustic phonon scattering. ⁷ No estimates have been made

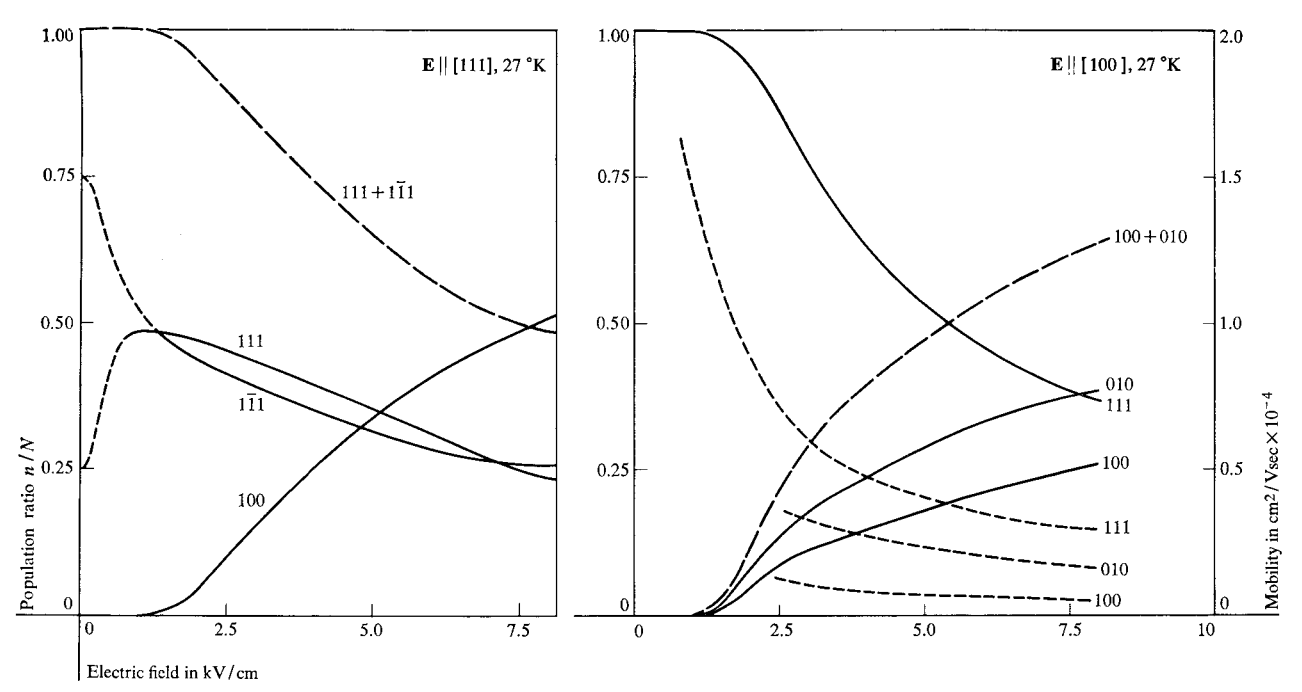


Figure 5 Variation of the fraction of the total number of carriers in the distinguishable sets of minima at $27^{\circ}K$ for E||[111] and E||[100] (full curves). The long-dash curves show the combined contributions of minima that are equivalent when E is zero. The short-dash curves show variation of mobility.

of the importance of the first two of these possibilities for germanium. Regarding the third, we find that in the region of 3 kV/cm and above, a wide variation in the value of $\mathcal{E}_{\rm av}$ has little effect on the results. This reveals that the effect of intraband acoustic phonon scattering is small when the presence of the $\langle 100 \rangle$ minima is taken into account and strongly suggests that this intraband effect is not making a major contribution to the BNDC.

The present calculations do not preclude some contribution to the BNDC of n-type germanium by mechanisms listed here. What they do show unequivocably is that population of $\langle 100 \rangle$ minima must be taken into account in any meaningful calculation and that, with apparently realistic parameters, the main feature of the BNDC can be accounted for solely by the electron transfer mechanism to $\langle 100 \rangle$ minima.

Acknowledgments

This paper is based extensively on calculations performed jointly with W. Fawcett and we thank him for permission to quote from them.

References

 B. K. Ridley and R. G. Pratt, J. Phys. Chem. Solids 26, 11 (1965).

- B. J. Elliott, J. B. Gunn and J. C. McGroddy, Appl. Phys. Letters 11, 253 (1967).
- 3. D. M. Chang and J. G. Ruch, Appl. Phys. Letters 12, 111 (1968).
- 4. J. E. Smith, J. C. McGroddy and M. I. Nathan, Proc. 9th Int. Conf. on Phys. Semicond, Moscow 2, 950 (1969).
- 5. A. A. Kastalskii and S. M. Ryvkin, Proc. 9th Int. Conf. on Phys. Semiconductors, Moscow 2, 955 (1969).
- 6. W. Fawcett and E. G. S. Paige, Electronics Letters 3, 505 (1957).
- P. J. Melz and J. C. McGroddy, Appl. Phys. Letters 12, 321 (1968).
- P. N. Butcher and W. Fawcett, Proc. Phys. Soc. (London) 86, 1205 (1965).
- 9. E. G. S. Paige, Prog. in Semiconductors, Heywood 8, 202 (1964).
- 10. R. Stratton, Proc. Roy. Soc. A242, 355 (1957).
- 11. W. Fawcett and E. G. S. Paige, to be published.
- 12. A. D. Boardman, W. Fawcett and H. D. Rees, Solid State Commun. 6, 305 (1968).
- 13. D. Long, Phys. Rev. 120, 2024 (1960).
- 14. A. Jayaraman and B. B. Kosicki, Proc. 9th Int. Conf. on Phys. Semiconductors, Moscow 1, 53 (1969).
- M. Asche, B. L. Boichenko, W. M. Bondar and O. G. Sabej, Proc. 9th Int. Conf. on Phys. Semiconductors, Moscow 2, 793 (1969).
- 16. M. I. Nathan, Phys. Rev. 130, 2201 (1963).
- 17. V. Dienys and J. Pozhela, *Phys. Stat. Sol.* 17, 769 (1966).

Received April 11, 1969